Composites Research

Vol. 35, No. 6, 402-411 (2022)
DOI: http://dx.doi.org/10.7234/composres.2022.35.6.402
ISSN 2288-2103(Print), ISSN 2288-2111(Online)

Special Issue Paper

Modified Graphene Oxide-Based Adsorbents Toward Hybrid Membranes for Organic Dye Removal Application

Thi Sinh Vo*, Khin Moe Lwin*, Sun Choi, Kyunghoon Kim*†**

ABSTRACT: In this study, the channels-contained hybrid membranes have been fabricated through the incorporation of glass fibers and GO sheets (GO/glass fibers, GG), or a mixture of chitosan/GO (CS/GO/glass fibers, CGG), as hybrid membranes using in organic dye removal. The material properties are well investigated the terms in the morphological, chemical, crystal, and thermal characterizations for verifying interactions in their formed structure. These hybrid membranes have been fitted well in pseudo-second order and Langmuir models that are associated with chemical adsorption and a monolayer approach, respectively. The highest adsorption ability of methylene blue and methyl orange reached 59.40 mg/g and 229.07 mg/g (GG); and 287.47 mg/g and 252.91 mg/g (CGG), which is more enhanced than that of previous GO-based other adsorbents. Moreover, the dye separation on these membranes could be favorable to superb sealing and trapping dye molecules from water instead of only the dye connection occurring on their surface, regarding the physically sieving effect. The membranes can also be reused within two and three adsorbing-desorbing cycles on the GG and CGG ones, respectively. These membranes can become future adsorbents to be applied for wastewater treatment due to their structural features.

Key Words: Graphene oxide, Organic dye, Composite membrane, Recyclability

1. INTRODUCTION

Current situations of industrial, domestic, and, agricultural waste effluents in water sources have caused a sharp increase in toxic pollutants [1]. Especially for organic dyes-contained water/wastewater, these dyes have been used in numerous industrial fields, and hence gravely influence current environmental issues. Most organic dye molecules contain aromatic rings in their structure, inducing highly toxic, carcinogenic, non-biodegradable, and mutagenic features in both aquatic and human lives. Therefore, a challenge for scientists on how to remove or minimize the organic dyes from water/wastewater was being proposed significantly [2,3]. Although plenty of various technologies have been well applied for removing dyes from water/wastewater, the whole cost is considered a major limitation of these technologies [2, 3]. Particularly, adsorption is one of the effective and simple techniques in organic dye-contaminated wastewater treatment, mainly thanks to low-cost, flexibility, simple design, and easy operation.

Besides, material systems have been greatly used in different research fields, especially for composite membrane-like materials [1,4]. A combination of two materials with various physical and chemical properties can form a functional composite material which is specialized to apply a certain purpose. For composite membranes, their result as effective adsorbents are able to have some remarkable features, i.e., chemical, physical, and interface properties, so the proposed preparation process and materials can be one of the important demands for researchers [3] to find the available, promising, economical and effective materials-based adsorbents. Hence, the exploitation of more effective and durable adsorbents for the controlled removal of organic dyes from wastewater sources is of great significance in environmental engineering.

Received 29 October 2022, received in revised form 28 November 2022, accepted 16 December 2022

*School of Mechanical Engineering, Sungkyunkwan University, Suwon 16419, Republic of Korea
**Centers for Environment, Health, and Welfare Research, Korea Institute of Science and Technology, Seoul 02792, Republic of Korea;
Division of Energy & Environment Technology, Korea University of Science and Technology (UST), Daejeon 34113, Republic of Korea
†Corresponding author (Email: kenkim@skku.edu)

To date, graphene oxide-based adsorbents (GO-based adsorbents) are being attracted much attention in recent years [5,6], owing to numerous specific groups on the GO nanosheets' surface. However, the only utilization of hydrophilic GO sheets is relatively low for dye removal performance, i.e., 17.3 mg/g (methylene blue), 2.47 mg/g (methyl violet), and 1.24 mg/g (Rhodamine B) [5], which is frequently modified or combined with other potential materials to enhance the removal performance and the stability of whole the modified structure [2-4]. Recent researches indicated that the dye removal performance of the adsorbents can be improved through binding and synthetic modification of GO sheets [7]. Terms in the binding sites improved stability, and the mechanical structure of the prepared materials provide a higher adsorption efficiency compared to the only use of GO sheets [2-4]. For that reason, the GO sheets can combine with a biopolymer through covalent or noncovalent interactions to create corresponding composites that serve as desirable adsorbents [2-4]. Among the natural biopolymers, chitosan (CS) component has been extensively applied in dye adsorption practices [4,8,9]; besides, it also has an enormous attention thanks to its excellent properties, serving as an ecofriendly material and a good adhesion [10]. The hydrogen bonds and covalent linkages occurring among oxygenated functional groups of the GO sheets and polysaccharide groups in the CS component are associated with the CS/GO composite's formation, as a stable and biocompatible composite with excellent thermal and mechanical thermal behaviors [4,8,9,11]. Further, glass fiber-contained membranes are excellent wettability and highly porous structures to be applied well in the polluted water/wastewater purifications [12,13]. Nonetheless, the use of glass fibers alone is very low in the dye adsorption performance, i.e., ~7.0 mg/g (methylene blue) [14]. The glass fibers can incorporate with other potential materials to improve the corresponding performance and be favorable for producing more stable structures, i.e., the GO sheets, and CS/GO mixtures.

Herein, the GO-based hybrid membranes will be prepared through incorporations of the glass fibers and the GO sheets (GO/glass fibers, GG membrane), or the mixture of CS/GO (CS/GO/glass fibers, CGG membrane), as hybrid membranes using in dye removal application, which can achieve proper and stable structural features to enhance their regeneration and recyclability. Besides the supporting channels (glass fibers) and the potential material sources, these GO-based hybrid membranes can be favorable for sealing and trapping the dye molecules that is thanks to the presence of specific groups and the physically sieving effect in whole the structure. Further, the whole approach of the preparation procedure is simple, using inexpensive and non-toxic materials, and thus can provide the potential demands to be scalable. To determine these, the morphological, chemical, crystal, and thermal features of the resultant hybrid membranes are also verified for the possibly formed interactions in the hybrid membranes-like adsorbents. The removal of methyl orange (MO) and methylene blue (MB) onto the hybrid membranes is clarified at various pH, adsorption periods, and dye concentrations, at the same time their adsorption and separation behaviors in the dye removal processes were also investigated specifically.

2. EXPERIMENTAL

2.1 Materials

Glass fibers-contained filtering membranes and GO dispersion are bought from a CHMLAB GROUP and a Grapheneall company, respectively. CS, MB, MO, acetic acid, and ethanol are bought from Sigma Aldrich.

2.2 Fabrication of hybrid membranes

CS solution is prepared by dissolving 1 g of CS in 100 mL of 2.5% (v/v) acetic acid and stirred overnight. GO dispersion is prepared with distilled water to 5 $g{\cdot}L^{-1}$ of concentration. The CS solution and GO dispersion are blended with each other according to an optional weight ratio of CS/GO (1/15, wt./wt.) [8], and then the CS/GO mixture is shaken violently for 10 secs to form an active hybrid network. Glass fiber membrane is cut in the rotary mill and sifted with a mesh size range of 0.2-0.5 mm (Seoul Korea standard testing sieve), and then are cleaned with distilled water and ethanol to remove residue parts. Next, the glass fibers are mixed with the material sources (GO dispersion, and CS/GO mixture) following an appropriate weight ratio of glass fibers/material source (1/10, wt./wt.) and stirred in a 20 mL-vial at room temperature (r.t.) for 24 h; afterward, the resultant solutions are sonicated for 5-10 min and poured into a 100 mm-petri dish containing a wipe paper sheet supporting. Finally, the resultant hybrid membranes (GG and CGG) are air-dried for 1-2 days.

2.3 Dye removal experiments

The stock dye solution is manufactured by directly dissolving dye molecules with estimated weights in distilled water. Then, the hybrid membrane (1×1 cm^2) is immersed into the prepared dye solution. Herein, various pH (3-11), dye concentrations (5-110 mg/L), and adsorption periods (0-250 min) are surveyed to evaluate the dye adsorption isotherms and kinetics onto the hybrid membrane-liked adsorbents, respectively. Concomitantly, the initial dye solution (C_o = 20 mg/L) is still considered to directly apply for the repeated adsorption experiments, which is meant to investigate the recyclability of the dye-adsorbed hybrid membranes. Specifically, the dye-adsorbed hybrid membranes are immersed in ethanol (~5 min) and filtered after each adsorption stage, and consequently, these dye-desorbed membranes are re-applied for the next procedure of adsorption experiments. The removal rate based on the change of dye concentration before and after adsorption [eqn. (1)], whereas the adsorption ability of dye on the

hybrid membranes is evaluated by eqn. (2). In which C_0 and C_e (mg/L) are the initial and equilibrium dye concentrations correspondingly; q (mg/g) is the adsorbed dye amount onto the hybrid membranes; V (L) is the initial volume of dye solution; and m (g) is considered as the mass of these hybrid membranes.

$$\text{Removal } (\%) = \frac{(C_0 - C_t)}{C_0} \times 100 \quad (1)$$

$$q = \frac{(C_0 - C_e) \times V}{m} \quad (2)$$

2.4 Analysis instruments

The membranes are captured from scanning electron microscopy (FE-SEM JSM-7600F) for determining their morphological features. Chemical characters are determined by an FT-IR analysis (Fourier-transform infrared spectroscopy), which is recorded by the spectrophotometer (Nicolet 380) and are scanned in a wavenumber range of 4000-500 cm^{-1}. To determine crystalline features, XRD (X-ray diffraction) analysis is performed and recorded at a 2θ range of 5-55° (D8 ADVANCE). Thermal properties are based on TG analysis (thermogravimetry) (TG/DTA6100), which is taken from 50°C and subsequently heated to 600°C at a heating rate of 20°C/min under the dry nitrogen atmosphere (20 mL/min). The dye solution was poured into a cuvette, and then a UV-visible spectrum is recorded on i9-UV/Vis spectrophotometer at r.t. (25 ± 2°C).

3. RESULTS AND DISCUSSION

3.1 Structural morphology

SEM captures are utilized to clarify the possibly formed interactions in the structure of hybrid membranes after completing incorporations of glass fibers and GO sheets (GG) or a CS/GO mixture (CGG). In Figs. 1(A-D), the glass fibers have acted as supporting channels, the GO sheets and the CS/GO mixture are considered hybrid bridges for readily connecting between the supporting channels and the hybrid bridges. A comparison of GG and CGG membranes in the structural features, the CS/GO bridges (Figs. 1B and 1D) are favorable for tightly adhering the supporting channels to each other instead of only the GO sheets (Figs. 1A and 1C), maybe owing to the entrance of CS support enhancing the extent of adhesion in whole the structure of CGG membrane. As such, the hybrid membranes prepared in this study can imply several possibly formed interactions between the glass fibers and the GO sheets, or between the glass fibers and the CS/GO mixture (Fig. 1E), i.e., hydrogen bonds. Besides, amide (-NHCO-) groups regarding a combination of the negatively charged GO sheets ($-COO^-$) and the positively charged CS ($-NH_3^+$) are also formed [Fig. 1E, (ii)], as demonstrated in our previous researches [4,8]. The CGG membrane has assembled a more stable hybrid network structure than the GG ones, and thus could considerably impact to the organic dye removal/separation ability and recyclability. More obviously, Figs. 1(A-D) indicate that the hybrid network of CGG membrane is observed through a tighter incorporation between these active

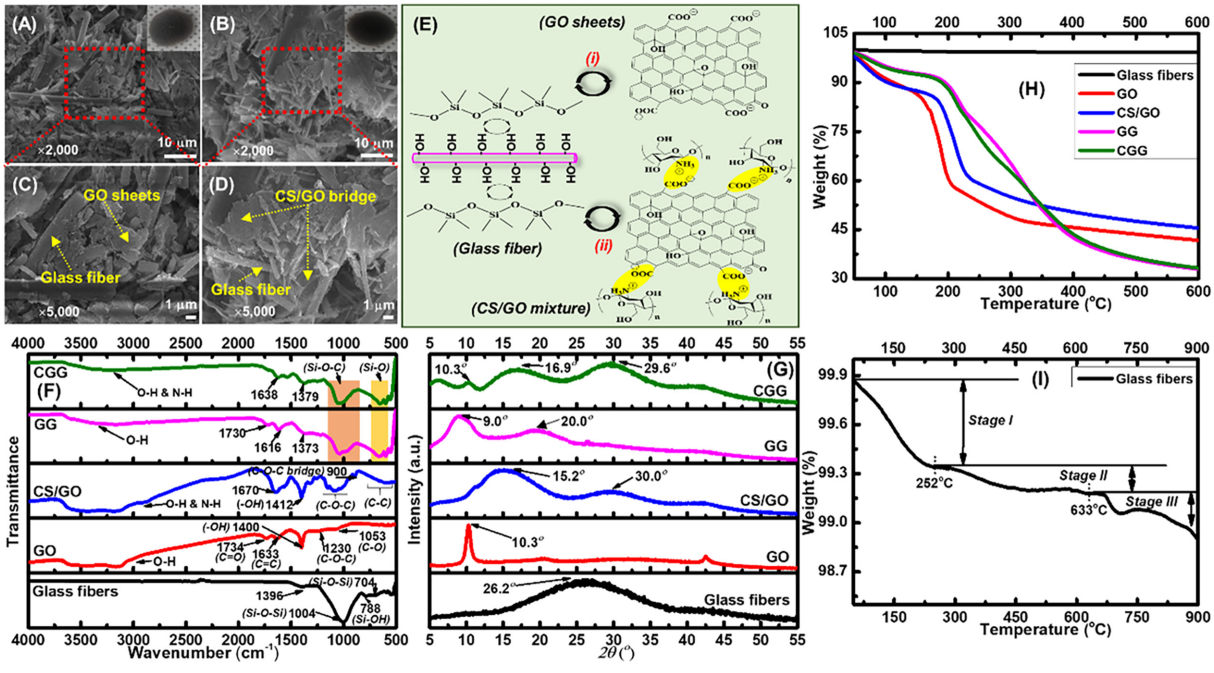

Fig. 1. SEM captures of GG (A, C) and CGG (B, D) membranes. Possible interactions in hybrid membranes (E): GG (i) and CGG (ii). FT-IR (F), XRD (G), and TG (H, I) curves of samples

materials under an air-drying condition comparing with that of GG one, significantly regarding the CS supporting component. This is meant for a good dispersion occurring among these active materials, i.e., GO sheets, CS, and glass fibers, instead of the only combination of GO sheets and glass fibers in the case of the GG membrane. The whole preparation process of the channels-contained hybrid membranes is performed simply by using low-cost materials, and hence, which can provide promising demands to be scalable, as well as successful combinations of the glass fibers and the GO sheets (GG) or the CS/GO mixture (CGG) in these processes.

3.2 Characterization

In FT-IR spectra (Fig. 1F), the typical peaks at 1004 cm^{-1} and 704 cm^{-1} are associated with the Si-O-Si stretching and bending vibrations in the glass fibers, respectively; besides, the ones at 1396 cm^{-1} and 788 cm^{-1} correspond to the BO_3^- (trigonal borate) and Si-OH stretching vibrations [15,16]. For the GO sheets, the main peaks at 1734 cm^{-1}, 1633 cm^{-1}, 1230 cm^{-1}, and 1053 cm^{-1} are contributed to the stretching vibrations of C=O (carboxyl group), C=C (aromatic ring), C-O-C (epoxy group) and C-O (alkoxy group) correspondingly; besides, the others at 3600-3000 cm^{-1} and 1400 cm^{-1} correspond to the -OH stretching vibration and deformation [4,8]. For the CS/GO mixture prepared in our previous study, the characteristic peaks of -OH/-NH, C=N/C=C, -OH, C-O-C, and C-C stretching vibrations are clearly observed at 3600-3000 cm^{-1}, 1670 cm^{-1}, 1187-1027 cm^{-1}, and 697-654 cm^{-1}, respectively. After conducting the incorporations between the glass fibers and the material sources (GO sheets or CS/GO mixture), the typical peaks of glass fibers are also revealed in both the GG and CGG, i.e., the Si-O stretching/bending vibrations (yellow column in Fig. 1F), and the BO_3^- stretching vibrations (1373 cm^{-1}/GG and 1379 cm^{-1}/CGG), especially for the newly formed Si-O-C vibrations (orange column in Fig. 1F); moreover, the typical peaks of material sources (GO sheets or CS/GO mixture) are seen at 3600-3000 cm^{-1}, 1730 cm^{-1}, 1616 cm^{-1} and 1638 cm^{-1} regarding the stretching vibrations of -OH/-NH, C=O, C=C, and C=N/C=C, correspondingly. Overall, these peaks have lightly displaced to the lower wavenumber regions compared to those of raw materials (i.e., glass fibers, GO sheets, and CS/GO mixture), indicating that there are complex interactions of the glass fibers and the material sources occurred in the whole the as-obtained structure of hybrid membranes. As such, the whole preparation process of the GO-based hybrid membranes is conducted simply through the use of inexpensive materials and thus can provide potential demands to be scalable, as well as successful combinations of the glass fibers and the GO sheets (GG membrane) or the CS/GO mixture (CGG membrane) in these processes.

XRD patterns of the hybrid membranes are also analyzed, as illustrated in Fig. 1G. In the glass fibers, the broad peak has appeared at 26.2° regarding to a region of silicate crystal [17]. Whereas, the characteristic peaks of GO sheet (10.3°) and CS/GO mixture (15.2° and 30.0°) are associated with the GO sheets' distance and the dense packing in the main chain of CS/GO, respectively. After performing the incorporations between the glass fibers and the material sources, the broad peaks at 9.0° and 20.0° are distinctly observed in the GG, as well as those of CGG are revealed at 10.3°, 16.9° and 29.6°, suggesting an effective combination of the glass fibers and the material sources. In another word, it probably involves to inter-molecular crystal inducing to reducing the possible movements of molecules and thus limited crystallization, which is also appropriate with the above results of SEM and FT-IR.

Besides the above-mentioned characterizations, the thermal features of as-obtained hybrid membranes have been also analyzed, as illustrated in Figs. 1H and 1I. It reveals that the first weight loss at ~100°C corresponds to the moisture and residual solvent in all samples [4,8]. The main weight loss of GO sheets is seen at 190°C, while that of the CS/GO mixture is at 213°C regarding the pyrolysis of the oxygen-contained GO sheets and CS molecules (Fig. 1H). For the glass fibers (Fig. 1I), there are three stages occurred in whole thermal decompositions [13]. Specifically, the low temperature of the first stage at 50-252°C is associated with the weight loss of residual solvent and absorbed water, while the second stage at 252-633°C is the condensation of ≡Si-OH groups [13]. The third stage of weight loss is observed at >633°C corresponding to the decomposition of $-CH_3$ groups in the glass fibers' structure; besides, the oxidation of $Si-CH_3$ groups is also occurred in this third stage (a dramatic exothermic peak at 703°C) [13]. After conducting the incorporations between the glass fibers and the material sources (GO sheets or CS/GO mixture), the main weight losses of GG and CGG are observed clearly at 249°C and 278°C (Fig. 1H), respectively, implying to the structural decomposition. Thereby, the hybrid membranes reached more stability in the thermal property compared to those of raw material sources (i.e., 190°C - GO sheets and 213°C - CS/GO mixture). Also, this result maybe reveal the possibly created interactions of the glass fibers and the material sources occur in whole the as-obtained structure of hybrid membranes, and is favorable for offering further in the above-analyzed results of SEM, FT-IR, and XRD. Overall, the molecular interactions of the GO-contained hybrid network reached the desirable features of the GO-based hybrid membranes, which can be favorable for the organic dye removal ability and structural durability of these hybrid membranes.

3.3 Dye removal ability

With the existence of aromatic rings in the MB and MO molecules, adsorption is favorable on the surface of hybrid membranes via π-π interaction [4,8,9]. To preliminary investigate the dye removal ability of the hybrid membranes, it is submerged into a dye-contained vial (20 mg/L), and its color

reliably turned to a brighter one after 150 min (Digital pictures are added in Figs. 2A and 2B). Also, the solution is expressed by using a i9-UV/Vis spectrophotometer (Figs. 2A and 2B), resulting that the typical absorbance peaks (666 nm/MB and 465 nm/MO) of organic dyes dropped drastically in their intensity after adsorption of 150 min onto the hybrid membranes (Figs. 2A and 2B). In both the MB and MO solutions, the CGG membrane has reached lower intensities of absorbance peaks compared with the GG one during this preliminary investigation. From the visual observations, both the GO-based hybrid membranes contained potential specific groups and physical traps to well serve for organic dye adsorption, especially for the CGG membrane.

Additionally, the pH approach in organic dye solution is also concerned as a great factor during the adsorption phenomenon, which significantly relates to the protonation of the specific groups and the surface charge of the GO-based hybrid membranes. Herein, the pH is investigated within a range of 3-11 to evaluate the changes in dye removal ability (t = 150 min and C_{dye} = 20 mg/L) of these hybrid membranes. Fig. 2C demonstrates the dye removal efficiency on the GG and CGG membranes, regard with the various pH values of the dye solution. Obviously, the MB removal rate increases sharply as the pH values increase from 3 to 6. Afterward, a steadily slow increase is seen at the following pH values (6 to 11) for both the GG and CGG membranes. Meanwhile, both these hybrid membranes have an opposite trend to the MO removal rate with increasing pH values. In another word, the MO removal rate slightly increases when these pH values rise from 3 to 6, after it drops down with the following pH values (6 to 11) onto both these membranes. As a result, the pH value of the organic dye solution is chosen at ~6 to apply directly for the next adsorption studies; particularly, this is meant to be close to the water medium. Obviously, the dye removal rate of the CGG membrane is higher than that of the GG one, meaning that the dye removal efficiency onto the CGG membrane has enhanced more than that of the GG one, regard with the addition of CS supporting component.

In general, the adsorption process regards to the protonated/deprotonated functional groups of the GO-based hybrid membranes with an ionic interaction of the anionic MO or the cationic MB. It can be obtained from the active material sources used in the GO-based hybrid membranes: (i) opened epoxy ring, and hydroxyl and carboxyl groups of the GG and CGG membranes originated from the GO sheets, (ii) amino groups of the CGG membrane originated from the CS component, (iii) the amide groups of the CGG membrane created after the chemical binding ability of the amino groups of the CS component with the carboxyl groups of the GO sheets. More specifically at lower pH values, the protonated functional groups contained in the CGG membrane have caused an electrostatic repulsion with the cationic MB leading to thwarting the MB adsorption manner, whereas these groups in the CGG membrane are able to give an electrostatic attraction with the anionic MO facilitating for the MO adsorption. Hence, the MB adsorption occurring at this condition is able to involve to interactions of van der Waals force or π-π stacking between the MB aromatic ring and the GO sheets. In another case at higher pH values, the oxygenated functional groups including carboxyl and groups of the GO sheets in both the GO-based hybrid membranes can be deprotonated and cause an appropriate electrostatic attraction with the cationic MB, whereas this trend is contrary to the anionic MO approach [4,8,9].

To further confirm details, the adsorption investigations are constructed on the GO-based hybrid membranes for removing various organic dyes from water. Particularly, the investigations of adsorption periods (0-250 min) and organic dye concentrations (5-110 mg/L) on the hybrid membranes are preformed to evaluate the dye removal ability (Figs. 1D and 1E). The dye removal ability rapidly increases within an initial 150 min of adsorption, and then which is relatively stable, suggesting that a dye adsorption rate occurs rapidly onto the hybrid membranes. In another investigation, the removal rate has dropped slightly in an initial dye concentration range of 5-20 mg/L of initial dye concentrations on both the GG and CGG, and then it reduces dramatically in a range of 20-110 mg/L. Thereby, the 150 min of adsorption and 20 mg/L of initial dye concentration are used for the next adsorption studies. Simultaneously, the dye removal rate of CGG membrane has reached better than that of GG one in both the above-mentioned investigations, suggesting that the dye removal ability is associated with the structural features and functional groups in these hybrid membranes. It means that the existence of CS support in the CGG membrane has enhanced the linking of the dye molecules and the specific groups contained in CGG one [4,8,9]. In addition, the MB removal ability is so much efficient more than that of MO by using these GO-based hybrid membranes, maybe due to the number of adsorptive sites contained in the hybrid membranes and the effect of steric hindrance contained in dye molecules leading to limiting the potential interaction extents between them.

3.3.1 Adsorption kinetics

The adsorption approach is a physicochemical procedure and occurred at the surface or interface positions, which involves to mass transfer of a solution from the liquid stage to the surface of adsorbents. In this study, the dye adsorption is measured at different adsorption periods (r.t.) and 20 mg/L of dye solutions. The adsorption capacity of dye onto the hybrid membranes is analyzed according to the eqn. (2), and the adsorption kinetic study has based on two models, i.e., pseudo-first and pseudo-second orders, which are calculated through linearized forms corresponding to eqns. (3) and (4). In which q_e and q_t (mg/g) are the adsorbed dye amounts at an equilibrium and an adsorption time (min), while k_1 and k_2 are

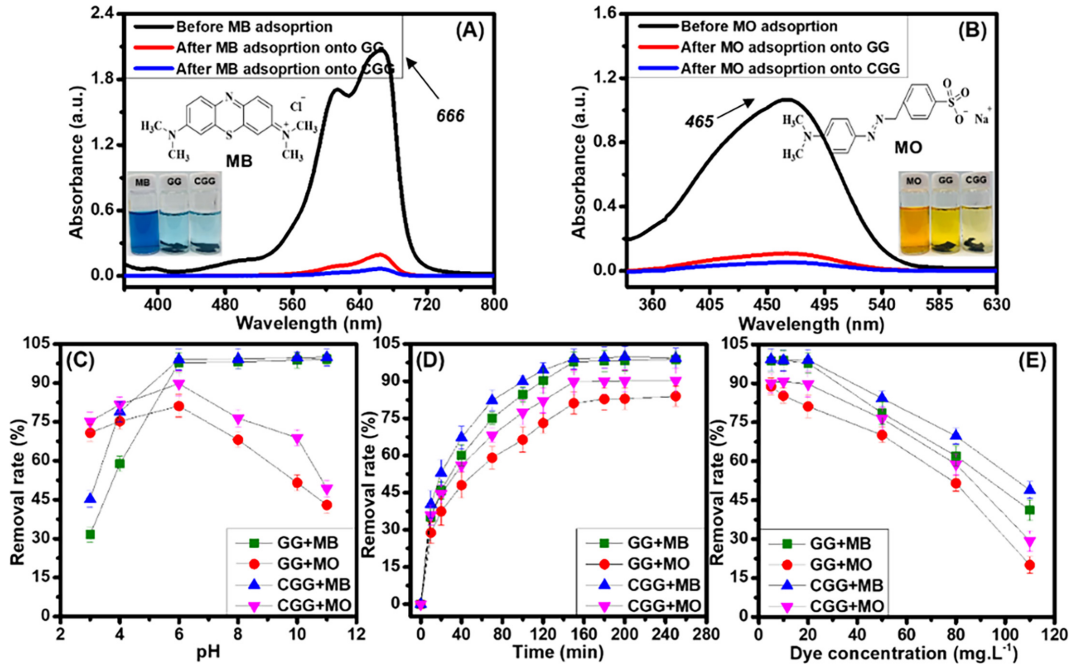

Fig. 2. UV-Vis curves of samples before and after MB (A) and MO (B) adsorption. Digital pictures showed the colorable changes of the dye solution before (one vial on the left side) and after adsorption (two vials on the right side). Adsorption studies of hybrid membranes at various pH values (C), adsorptive periods (D), and dye concentrations (E)

the rate constants of pseudo-first and pseudo-second order models, respectively.

$$\frac{1}{q_t} = \frac{k_1}{q_e \times t} + \frac{1}{q_e} \tag{3}$$

$$\frac{t}{q_t} = \frac{1}{k_2 \times q_e^2} + \frac{1}{q_e} \times t \tag{4}$$

According to the above-mentioned models (Figs. 3A and 3B), the reached parameters have been listed in Table 1, resulting that the R^2-correlation coefficients of the pseudo-second order are almost near 0.9999 than those of the pseudo-first order for both the hybrid membranes and the experimental ones ($q_{e,\,exp}$) are also similar with the calculated values of q_e ($q_{e,\,cal}$) in case of the pseudo-second order. Therefore, the dye adsorption process occurring in these hybrid membranes is attributed to chemical adsorption, and this suitable model has also been reported in previous GO-based adsorbents [18-23]. Further, the adsorption abilities ($q_{e,\,exp}$, and $q_{e,\,cal}$) of the CGG membrane are greater than those of the GG one for adsorbing MB and MO, maybe on account of the structural features and specific groups in this hybrid membrane being favorable for sealing and trapping dye molecules in whole the structure of the CGG membrane.

3.3.2 Adsorption isotherms

Studies of adsorption isotherm are conducted to analyze the reliable relationship between amounts of adsorbed dye on the surface of adsorbents with the per unit weight and the dye concentrations. Herein, the dye adsorption has been measured at 150 min of adsorption period (r.t.) and a tested dye concentration range of 5-110 mg/L. Two isotherm models, i.e., Langmuir and Freundlich, are used to verify mechanistic parameters regarding the dye adsorption process, calculated through linearized forms corresponding to eqn. (5) and eqn. (6). In which C_e (mg/L) is the equilibrium concentration of tested dye solutions; q_e and q_m (mg/g) are attributed to absorption at equilibrium and the highest adsorption abilities correspondingly; K_L and K_F are the isotherm constants of the Langmuir and Freundlich models respectively, and n is the heterogeneity factor.

$$\frac{C_e}{q_e} = \frac{1}{q_m \times K_L} + \frac{C_e}{q_m} \tag{5}$$

$$\log(q_e) = \log(K_F) + \frac{1}{n}\log(C_e) \tag{6}$$

Through these models, the model parameters have achieved (Figs. 3C and 3D), resulting that the R^2-correlation coefficient has obtained to be closer to 0.999 from the calculated bases of the Langmuir model comparing with that of Freundlich one (Table 1). As such, the Langmuir model is more consistent with the adsorption features of MB and MO onto the hybrid membranes, and thus the adsorption process is occurred in a monolayer manner, regarding the formation of adsorbed dye molecules-contained thin blocking on the surface (outside

surface) of these hybrid membranes. Also, this appropriate model has been revealed in previous GO-based adsorbents [18-22]. At the same time, the highest adsorption ability of MB and MO onto the hybrid membranes has reached 259.40 mg/g and 229.07 mg/g (GG); and 287.47 mg/g and 252.91 mg/g (CGG), correspondingly. As such, the CGG membrane has improved better than the GG one in the dye adsorption, owing to the structural features and specific groups in this hybrid membrane being favorable for sealing and trapping dye molecules in whole the structure of the CGG hybrid membrane. These are as above-discussed in the SEM results, meaning that the proposed combination of the glass fibers and the active materials has provided physical traps (as neighboring voids), which are constructed after blending and air-drying them. Further, the highest adsorption ability of these hybrid membranes is relatively greater than that of other relevant absorbents [18,22,23], which can become future adsorbents for dye removal applications.

3.4 Dye flux and rejection

In addition, the dye solution of 20 mg/L is still applied for the separation process, which is performed at low pressure, using a vacuum suction machine (0.09 MPa, r.t.). Based on a liquid volume (V), a specified time (t), and a membrane's area (A, 3.14 cm^2), the flux [J, L/(m^2×h)] could be reached by calculating in eqn. (7) for removing dye on these membranes. Besides, the rejection (R, %) is calculated from eqn. (8), relating to the permeated (C_p) and fed (C_f) concentrations of dye solution. To effectively fix the hybrid membranes on the testing platform, a vacuum suction flask and funnel system has used to probably facilitate for separation procedures. In that manner, the hybrid membranes are fixed tightly by placing the funnel on the flask with the help of a gasket and supporting disc. The down edge of the funnel has been placed on the hybrid membrane and tightened. Therefore, there was no leakage between the hybrid membrane and the funnel.

$$J = \frac{V}{A \times t} \tag{7}$$

$$R(\%) = \frac{C_f - C_p}{C_f} \times 100 \tag{8}$$

In Figs. 3E and 3F, the dye flux and rejection values of CGG are higher than those of GG in both MB and MO separations, i.e., 95.0 $L{\cdot}m^{-2}{\cdot}h^{-1}$ and 80.0% (GG, MB); 95.6 $L{\cdot}m^{-2}{\cdot}h^{-1}$ and 81.0% (GG, MO); 99.7 $L{\cdot}m^{-2}{\cdot}h^{-1}$ and 85.3% (CGG, MB); 101.2 $Lm^{-2}{\cdot}h^{-1}$ and 85.0% (CGG, MO). These reveal that the separation ability of the hybrid membranes is significantly associated with the structural features (as described in SEM analysis) and the CS support in the CGG membrane for enhancing the dye flux and rejection performances, which have improved the resistance of dye molecules permeating the GO-based membrane. Overall, the especially structural features and numerous specific groups in the hybrid membranes are favorable for readily linking the dye molecules and the functional groups (hydrogen bonds, electrostatic interactions, π-stacking, etc.), or serval traps and gaps contained in the structural morphology to well remove dye molecules from water [5]. In addition to π-π stacking (aromatic rings) among the dye molecules and the hybrid membranes [4,8], the case of MO removal (anionic dye) from water indicates strong electrostatic interactions by using the CGG, thanks to the availably positive charges (-NH_3^+) in the CS support component, while the extent of electrostatic interactions is better for the case of MB removal (cationic dye) of the GG regarding the negative charges (-COO^-) in the GO sheets. Further, the van der Waals and hydrogen bonds can exist in the dye adsorption approach [24]. The removal ability of MB is so much efficient more than that of MO by using the as-obtained hybrid membranes, which involves the number of adsorptive sites contained in the hybrid membranes and the effect of steric hindrance contained in dye molecules that could limit the potential inter-

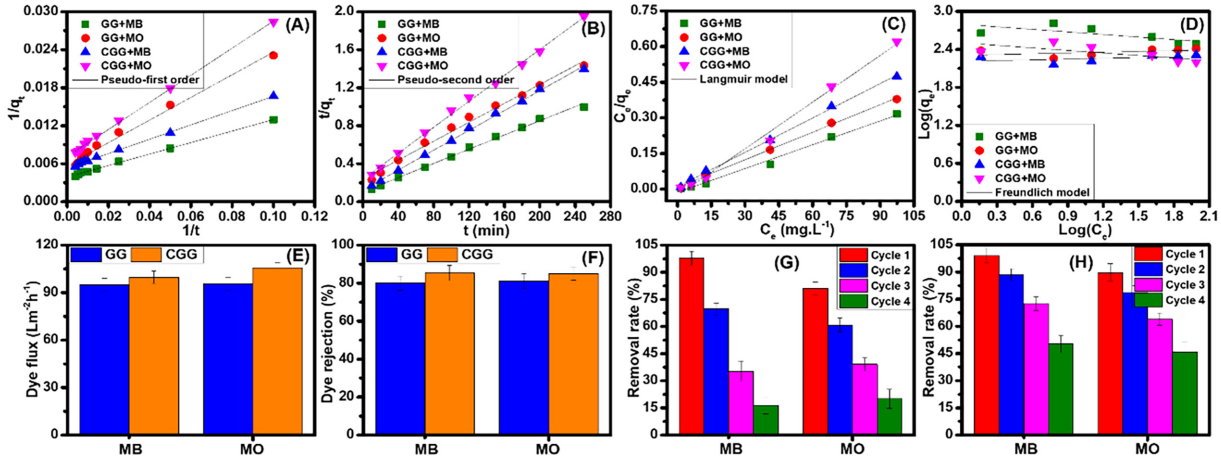

Fig. 3. Kinetic (A, B), isotherm (C, D) models, dye flux (E), and rejection (F) of the hybrid membranes. Recyclability of the dye-adsorbed GG (G) and CGG (H) membranes

action extents among them. Additionally, the dye separation ability on these channels-contained hybrid membranes could be associated with the electronegativity of ions and the physically sieving effect to well seal and trap the dye molecules from water instead of only the dye connection occurring on the surface of hybrid membranes [25,26], owing to the existence of glass fibers (as channels) in the hybrid membranes. Concomitantly, large dye molecules could be also blocked and kept easily in the especial structure of the GO-based hybrid membranes to achieve the admirable separation ability. With stability of structural features and numerous specific groups, these hybrid membranes have reached quite well in organic dye adsorption and separation applications.

3.5 Recyclability

Herein, a solvent with safe and economic utilization is applied for desorbing organic dye molecules from the dyes-adsorbed hybrid membranes, i.e., ethanol, and then they are air-dried to parrot the following adsorption procedure. In Figs. 3G and 3H, the removal rate of the GG membrane is well maintained within the initial two cycles for removing MB and MO molecules corresponding to 97.8-69.7% and 81.1-60.9%, while that of the CGG membrane is significantly stable within the initial three cycles, i.e., 99.0-72.5% (MB) and 89.7-63.9% (MO). Concomitantly, the MB and MO removal rates have significantly dropped to third and fourth cycles corresponding to the GG and CGG membranes, i.e., 35.4% (GG, MB); 39.1% (GG, MO); 50.2% (CGG, MB) and 45.8% (CGG, MO). In the approach of recycling performance, it showed that the adsorption-desorption cycles are quite low. This is meant to reach a significant decrease in the recycling performance of both membranes, regarding with the structural durability of the active networks that existed in the hybrid membranes. The interactions of the active materials in the hybrid membranes can become weak to probably separate each other after the desorption process, which impacts to a decrease in the potential groups and stability of active sites in the whole of the hybrid membrane structure. However, both the GG and CGG membranes resulted a quite good removal ability during the recycling produce, this removal efficiency of the CGG membrane obtained greater much than that of the GG one in recyclability, thanks to the especially structural morphology and the CS supporting component in the CGG membrane. In general, the durability of the hybrid membranes probably accepts in the recyclability, and thus lowers a little bit to the costs and becomes future adsorbents for dye removal applications.

Table 1. Kinetic and isotherm parameters for dye adsorption onto the hybrid membranes

Models	Parameters	GG		CGG	
		MB	MO	MB	MO
Pseudo-first order	$q_{e,\,exp}$	225.19	189.65	256.41	239.06
	k_1	23.29	31.17	21.13	30.01
	$q_{e,\,cal}$	206.42	174.22	209.92	200.25
	R^2	0.9970	0.9885	0.9977	0.9972
Pseudo-second order	$q_{e,\,exp}$	225.19	189.65	256.41	239.06
	$k_2\times10^{-4}$	1.33	1.03	2.19	1.95
	$q_{e,\,cal}$	237.38	201.21	261.57	246.63
	R^2	0.9972	0.9991	0.9989	0.9988
Models	Parameters	GG		CGG	
		MB	MO	MB	MO
Langmuir	K_L	0.25	0.58	0.47	0.61
	R^2	0.9909	0.9982	0.9988	0.9912
	q_m	259.40	229.07	287.47	252.91
Freundlich	n	7.44	24.43	24.38	7.44
	R^2	0.6083	0.7803	0.8413	0.7094
	K_F	6.17	4.44	6.91	5.46

4. CONCLUSIONS

In summary, the hybrid membranes containing the supporting channels and specific groups are well fabricated through the incorporations among the glass fibers (as supporting channels) and the active material sources (i.e., GO sheets and CS/GO mixture), assembling the proper and stable structures and considerably influencing to the organic dye removal ability and recyclability. Further, the characterization analysis also revealed that quite complex interactions are formed in the whole of the attained structure of these hybrid membranes. The hybrid membranes reached a high removal ability for both MB and MO, especially for the CGG membrane. Simultaneously, the removal ability has reached a proper degree in MB removal compared with MO one among these membranes, which involved to the number of adsorptive sites contained in the membranes and the effect of steric hindrance contained in dye molecules that could limit the potential interaction extents among them. In the adsorption kinetic and isotherm studies, the adsorption is appropriate with the pseudo-second order and Langmuir models, mainly regarding chemical adsorption and a monolayer approach, correspondingly. Also, the highest adsorption ability of dyes on the as-prepared hybrid membranes is better than that of other relevant GO-based adsorbents. Instead of only the dye connection occurring on the surface of hybrid membranes, the dye separation ability on the membranes could be favorable to well seal and trap the dye molecules from water, thanks to the channels-liked glass fibers in these hybrid membranes, as the physically sieving effect. Although the number of adsorbing-desorbing cycle is quite low, recyclability could reach an acceptable result for the system of hybrid membranes-like adsorbents applied in dye removal application, which is maintained quite well to two and three adsorbing-desorbing cycles corresponding to the GG and CGG membranes. Thereby, the

hybrid membranes can be promising candidates to be used for wastewater treatment, on account of proper structural features, numerous specific groups, and simple operation.

ACKNOWLEDGMENT

This work was supported by the National Research Foundation of Korea (NRF) grant funded by the Korea government (MSIT) (NRF-2020R1A2C4002557) and KIST institutional grant (KIST 2E31931).

REFERENCES

1. Vo, T.S., Hossain, M.M., Jeong, H.M., and Kim, K., "Heavy Metal Removal Applications Using Adsorptive Membranes", *Nano Convergence*, Vol. 7, No. 1, 2020, pp. 1-26.
2. Pereira, A.G.B., Rodrigues, F.H.A., Paulino, A.T., Martins, A.F., and Fajardo, A.R., "Recent Advances on Composite Hydrogels Designed for the Remediation of Dye-contaminated Water and Wastewater: A Review", *Journal of Cleaner Production*, Vol. 284, 2021, pp. 124703.
3. Alves, D.D.C., Healy, B., Pinto, L.A.D., Cadaval, T.R.S., and Breslin, C.B., "Recent Developments in Chitosan-Based Adsorbents for the Removal of Pollutants from Aqueous Environments", *Molecules*, Vol. 26, No. 3, 2021, pp. 594.
4. Vo, T.S., Hossain, M.M., Lim, T., Suk, J.W., Choi, S., and Kim, K., "Graphene Oxide-Chitosan Network on a Dialysis Cellulose Membrane for Efficient Removal of Organic Dyes", *ACS Applied Bio Materials*, Vol. 5, No. 6, 2022, pp. 2795-2811.
5. Ramesha, G.K., Kumara, A.V., Muralidhara, H.B., and Sampath, S., "Graphene and Graphene Oxide as Effective Adsorbents Toward Anionic and Cationic Dyes", *Journal of Colloid and Interface Science*, Vol. 361, No. 1, 2011, pp. 270-277.
6. Zhu, L., Guo, X., Chen, Y., Chen, Z., Lan, Y., Hong, Y., and Lan, W., "Graphene Oxide Composite Membranes for Water Purification", *ACS Applied Nano Materials*, Vol. 5, No. 3, 2022, pp. 3643-3653.
7. Park, S., Lee, K.S., Bozoklu, G., Cai, W., Nguyen, S.T., and Ruoff', R.S., "Graphene Oxide Papers Modified by Divalent Ions - Enhancing Mechanical Properties via Chemical Cross-linking", *ACS Nano*, Vol. 2, No. 3, 2008, pp. 572-578.
8. Vo, T.S., Vo, T.T.B.C., Suk, J.W., and Kim, K., "Recycling Performance of Graphene Oxide-chitosan Hybrid Hydrogels for Removal of Cationic and Anionic Dyes", *Nano Convergence*, Vol. 7, No. 1, 2020, pp. 1-11.
9. Vo, T.S., Hossain, M.M., Lim, T., Suk, J.W., Choi, S., and Kim, K., "Modification of the Interfacial Glass Fiber Surface Through Graphene Oxide-chitosan Interactions for Excellent Dye Removal as an Adsorptive Membrane", *Journal of Environmental Chemical Engineering*, Vol. 10, No. 6, 2022, pp. 108965.
10. Fan, L.L., Luo, C.N., Sun, M., Li, X.J., and Qiu, H.M., "Highly Selective Adsorption of Lead Ions by Water-dispersible Magnetic Chitosan/graphene Oxide Composites", *Colloids and Surfaces B-Biointerfaces*, Vol. 103, 2013, pp. 523-529.
11. Yang, X.M., Tu, Y.F., Li, L.A., Shang, S.M., and Tao, X.M., "Well-Dispersed Chitosan/Graphene Oxide Nanocomposites", *Acs Applied Materials & Interfaces*, Vol. 2, No. 6, 2010, pp. 1707-1713.
12. Yasui, K., Sasaki, K., Ikeda, N., and Kinoshita, H., "Dye Adsorbent Materials Based on Porous Ceramics from Glass Fiber-Reinforced Plastic and Clay", *Applied Sciences-Basel*, Vol. 9, No. 8, 2019, pp. 1574.
13. Zhou, T., Cheng, X.D., Pan, Y.L., Li, C.C., Gong, L.L., and Zhang, H.P., "Mechanical Performance and Thermal Stability of Glass Fiber Reinforced Silica Aerogel Composites Based on Co-precursor Method by Freeze Drying", *Applied Surface Science*, Vol. 437, 2018, pp. 321-328.
14. Chakrabarti, S., and Dutta, B.K., "On the Adsorption and Diffusion of Methylene Blue in Glass Fibers", *Journal of Colloid and Interface Science*, Vol. 286, No. 2, 2005, pp. 807-811.
15. Gautam, C., Yadav, A.K., and Singh, A.K., "A Review on Infrared Spectroscopy of Borate Glasses with Effects of Different Additives", *ISRN Ceramics*, Vol. 2012, 2012, pp. 1-17.
16. Saravanakumar, K., Arumugam, V., Souhith, R., and Santulli, C., "Influence of Milled Glass Fiber Fillers on Mode I & Mode II Interlaminar Fracture Toughness of Epoxy Resin for Fabrication of Glass/Epoxy Composites", *Fibers*, Vol. 8, No. 6, 2020, pp. 36.
17. Guo, W., and Ruckenstein, E., "Modified Glass Fiber Membrane and Its Application to Membrane Affinity Chromatography", *Journal of Membrane Science*, Vol. 215, No. 1-2, 2003, pp. 141-155.
18. Sirajudheen, P., Karthikeyan, P., Ramkumar, K., and Meenakshi, S., "Effective Removal of Organic Pollutants by Adsorption onto Chitosan Supported Graphene Oxide-hydroxyapatite Composite: A Novel Reusable Adsorbent", *Journal of Molecular Liquids*, Vol. 318, 2020, pp. 114200.
19. Guo, X.Q., Qu, L.J., Tian, M.W., Zhu, S.F., Zhang, X.S., Tang, X.N., and Sun, K.K., "Chitosan/Graphene Oxide Composite as an Effective Adsorbent for Reactive Red Dye Removal", *Water Environment Research*, Vol. 88, No. 7, 2016, pp. 579-588.
20. Li, L., Fan, L., Duan, H., Wang, X., and Luo, C., "Magnetically Separable Functionalized Graphene Oxide Decorated with Magnetic Cyclodextrin as an Excellent Adsorbent for Dye Removal", *RSC Advances*, Vol. 4, No. 70, 2014, pp. 37114-37121.
21. Ma, T., Chang, P.R., Zheng, P., Zhao, F., and Ma, X., "Fabrication of Ultra-light Graphene-based Gels and Their Adsorption of Methylene Blue", *Chemical Engineering Journal*, Vol. 240, 2014, pp. 595-600.
22. Deng, J.-H., Zhang, X.-R., Zeng, G.-M., Gong, J.-L., Niu, Q.-Y., and Liang, J., "Simultaneous Removal of Cd (II) and Ionic Dyes from Aqueous Solution Using Magnetic Graphene Oxide Nanocomposite as an Adsorbent", *Chemical Engineering Journal*, Vol. 226, 2013, pp. 189-200.
23. Fan, L., Luo, C., Sun, M., Li, X., Lu, F., and Qiu, H., "Preparation of Novel Magnetic Chitosan/graphene Oxide Composite as Effective Adsorbents Toward Methylene Blue", *Bioresource Technology*, Vol. 114, 2012, pp. 703-706.
24. Balapanuru, J., Yang, J.X., Xiao, S., Bao, Q.L., Jahan, M., Pola-

varapu, L., Wei, J., Xu, Q.H., and Loh, K.P., "A Graphene Oxide-Organic Dye Ionic Complex with DNA-Sensing and Optical-Limiting Properties", *Angewandte Chemie-International Edition*, Vol. 49, No. 37, 2010, pp. 6549-6553.

25. Bai, L.M., Liu, Y.T., Ding, A., Ren, N.Q., Li, G.B., and Liang, H., "Fabrication and Characterization of Thin-film Composite (TFC) Nanofiltration Membranes Incorporated with Cellulose Nanocrystals (CNCs) for Enhanced Desalination Performance and Dye Removal", *Chemical Engineering Journal*, Vol. 358, 2019, pp. 1519-1528.
26. Ma, F.F., Zhang, D., Zhang, N., Huang, T., and Wang, Y., "Polydopamine-assisted Deposition of Polypyrrole on Electrospun Poly(vinylidene fluoride) Nanofibers for Bidirectional Removal of Cation and Anion Dyes", *Chemical Engineering Journal*, Vol. 354, 2018, pp. 432-444.